CHALMERS
UNIVERSITY OF TECHNOLOGY

Dynamic Resource Allocation in Metro Elastic Optical Networks using Lyapunov Drift Optimization

Citation for the original published paper (version of record):
Hadi, M., Pakravan, M., Agrell, E. (2019). Dynamic Resource Allocation in Metro Elastic Optical Networks using Lyapunov Drift Optimization. Journal of Optical Communications and Networking, 11(6): 250-259. http://dx.doi.org/10.1364/JOCN.11.000250

Dynamic Resource Allocation in Metro Elastic Optical Networks using Lyapunov Drift Optimization

Mohammad Hadi, *Student Member, IEEE,* Mohammad Reza Pakravan, *Member, IEEE,* and Erik Agrell, *Fellow, IEEE*

***Abstract*—Consistent growth in the volume and dynamic behavior of traffic mandates new requirements for fast and adaptive resource allocation in metro networks. We propose a dynamic resource allocation technique for adaptive minimization of spectrum usage in metro elastic optical networks. We consider optical transmission as a service specified by its bandwidth profile parameters, which are minimum, average, and maximum required transmission rates. To consider random traffic events, we use a stochastic optimization technique to develop a novel formulation for dynamic resource allocation in which service level specifications and network stability constraints are addressed. Next, we employ the elegant theory of Lyapunov optimization to solve the stochastic optimization problem and derive a fast integer linear program, which is periodically solved to create an adaptation between available resources and dynamic network state. To quantize the performance of the proposed technique, we report its spectral efficiency as a function of peak to average traffic ratio and Lyapunov penalty coefficient. Simulation results show that the dynamic resource allocation procedure can improve spectral efficiency by a factor of 3.3 for a peak to average traffic ratio of 1.37 and a Lyapunov penalty coefficient of 10^3 in comparison with fixed network planning. There is also a trade-off between transmission delay and spectrum utilization in the proposed technique, which can be adjusted by a Lyapunov penalty coefficient.**

***Keywords*—Stochastic optimization, Lyapunov drift theory, Elastic optical networks, Metro Networks, Software-Defined Networking.**

I. Introduction

METRO networks have experienced a radical change over the past few years, primarily as a result of considerable traffic growth, of new traffic distribution patterns, and of new dynamics [1]. Traffic growth studies show that traffic is growing almost two times faster in the metro compared to the core networks [2], [3]. To improve end user performance, a large fraction of the services is being moved to data centers located inside the metro networks where the requesting end users belong. This reduces delivery latency, accelerates the change of traffic distribution and increases the amount of traffic terminated in the metro network [1], [4]. Metro networks are forecasted to account for about 70% of the total IP traffic in near future mostly due to an increasing trend towards content delivery networks [5]. Metro networks are expected to become the cornerstone of future technologies such as 5G, where network flows can vary in terms of duration, bandwidth, and delay profile requirements [1].

An efficient network scheduling can benefit from flexible data rate adjustment and dynamic allocation/release of the physical resources to match the actual size and duration of the data flows. This needs to transfer some of the network dynamics and flexibility from upper layer switching down to the physical layer. Such flexible scheduling deserves a growing focus and shows more promises than ever before due to the unprecedented growth and increasing dynamism of the traffic in metro networks [1], [6]. The growing acceptance of software-defined networking (SDN) and network function virtualization concepts has paved the way for the development of metro elastic optical networks (MEONs) by offering new high value services that operators can propose [4], [6], [7]. Optical network slicing, whereby a sub-network or a lightpath is customized and temporarily allocated to a given subscriber, securely and separately from the other subscribers, is one of these services. There is little doubt that the flexible optical layer under development today will do its share of the work, so that optical network slicing and more generally transport-as-a-service (TaaS) becomes a reality in MEONs [1], [4].

A metro network design can be implemented using technologies such as optical transport network (OTN) and elastic optical network (EON) [2]. OTN architectures would experience extensive optical-electronic-optical (OEO) conversions, which leads to high cost, high power consumption and increased connection latency due to electrical processes inside a node [2]. EONs were proposed to provide a scalable and competitive technology to support traffic growth and to make the main parameters of network elements tunable, in order to better match the delivered data rate to the actual needs. Two key enablers for EONs are coherent detection and digital signal processing which have been practically developed and deployed in todays flexible network elements [1], [6]. In EON, a direct lightpath is established for each connection request, which avoids the OEO conversions required in the OTN, and therefore can eliminate many intermediate OTN switches for lower hardware cost, and help reduce connection latency and system power consumption [8]. Another important fact is that to make fast reconfigurable MEONs a reality, hit-less elastic transponders become an important feature in the data plane [9]. Fortunately, zero-loss of data during the transponder reconfiguration has

M. Hadi and E. Agrell are with the Department of Electrical Engineering, Chalmers University of Technology, SE-41296 Gothenburg, Sweden (e-mails: mohadi@chalmers.se, eagrell@chalmers.se). M. R. Pakravan is with the Department of Electrical Engineering, Sharif University of Technology, 11365-11155 Tehran, Iran (e-mail: pakravan@sharif.edu). This work was supported in part by Vinnova under grant no. 2017-05228 and conducted in part while M. Hadi was with the Department of Electrical Engineering, Sharif University of Technology.

been practically demonstrated [8], [10], [11]. The reported maximum switching time of the proposed hit-less transponders is experimentally measured to less than 450 μs, a sufficiently fast duration for practical deployment of agile online resource allocation algorithms in MEONs [10], [12].

Lyapunov drift theory is successfully used for optimal control in dynamic communication and queuing systems where a typical goal is to stabilize all network queues while optimizing some performance objectives. In Lyapunov optimization, a nonnegative scalar measure of the network stability is added as a penalty term to the goal function and the solution of the problem is derived using the Min-Drift-Plus-Penalty algorithm [13].

Online resource allocation in MEONs is a promising research topic. Although resource allocation in core EONs has been extensively studied [14]–[16], dynamic resource allocation in MEONs needs more research [17]. The key point is that the proposed algorithms for core EONs cannot be readily applied to MEONs since they do not consider the requirements of metro networks such as dynamic traffic fluctuation, short reallocation period, and service differentiation [1], [18], [19]. The quality of service (QoS) is a necessary parameter for practical management of MEONs; however, there is no comprehensive research work on QoS-aware resource allocation for MEONs. In this paper, we focus on dynamic QoS-aware resource allocation for an MEON with TaaS capability. Each service has a bandwidth profile which is characterized by its minimum, average, and maximum transmission rate. We use stochastic optimization techniques to formulate a dynamic resource allocation problem that considers service level specifications and aims at minimization of the time-averaged spectrum usage to free up spectrum for incoming service requests. We then show how the Lyapunov drift theorem can be employed to solve the formulated stochastic optimization problem and guarantee the network stability [13]. We apply the Min-Drift-Plus-Penalty algorithm to derive an efficient integer linear program (ILP) that is periodically solved to create an adaptation between allocated resources and traffic demands. Simulation results show that the proposed procedure is sufficiently fast to satisfy the timing constraint of online resource allocation with a reallocation period of less than a few seconds. Such a fast algorithm can be used for network planning to estimate the steady state behavior of the network and determine the number of required devices such as the number of required flexible transponders in each node. To validate the performance of the proposed technique, we compare its results with fixed resource allocation in which the network is over-dimensioned for the worst-case traffic requirements. We use spectral efficiency as a performance metric to quantize the improvement of the technique and report its values in terms of time, peak to average traffic ratio, and Lyapunov penalty coefficient. Numerical results show that when peak to average traffic ratio and Lyapunov penalty coefficient are 1.37 and 10^3, respectively, our dynamic resource allocation procedure can improve spectral efficiency by a factor of 3.3. This means that for the same spectrum usage, the transmission capacity of our algorithm is 3.3 times greater than the transmission capacity of the fixed resource allocation method. The main reason behind this impressive improvement is that while service level agreements (SLAs) allow, the algorithm automatically postpones transmissions from high traffic time intervals to low traffic intervals to minimize spectrum usage, improve system efficiency, and enhance network capacity. According to the numerical results, there is a trade-off between transmission delay and spectral efficiency in the proposed formulation, which can be adjusted by the Lyapunov penalty coefficient.

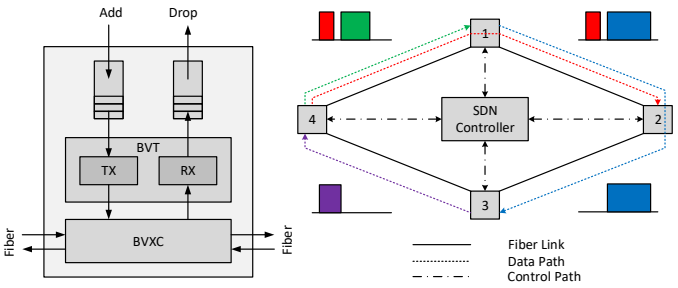

Fig. 1: System model assumptions for the metro elastic optical network. BVXC: Bandwidth-Variable Cross-Connect, BVT: Bandwidth-Variable Transponder.

The rest of the paper is organized as follows. The system model is introduced in Section II. In Sections III, we propose our formulation and use Lyapunov drift optimization to solve it. Simulation results are included in Section IV. Finally, we conclude the paper in Section V.

II. System Model

We consider an MEON characterized by an arbitrary topology graph that operates in discrete time slots $n \in \{0, 1, 2, \cdots\}$ with slot width $\mathcal{T}$. An illustrative network topology is depicted in Fig. 1. The optical fiber bandwidth $\mathcal{B}$ is divided into $\mathcal{F}$ equal-bandwidth frequency slots with a granularity of $\mathcal{W}$. Topology links consist of one amplifier at the input and another at the output in order to manage the power budget and enable a cascade of several links along a light-path. Fortunately, fiber links in MEONs are sufficiently short to enable optical transmission without intermediate amplification and/or regeneration [4], [20]. As shown in Fig. 1, each topology node is equipped with a buffer-less cross-connect and a bank of transponders to optically switch crossing light-paths and make add/drop operations for input/output traffic flows, respectively. Cross-connects and transponders are bandwidth-variable, which means that they can operate on an arbitrary contiguous set of spectrum slots. The required flexibility of the transponders and cross-connects can be achieved using different technologies such as optical orthogonal frequency division multiplexing, Nyquist wavelength division multiplexing, time-frequency packing, etc. [6] and, there is no constraint on the implementation technology in this work.

There can be one or multiple connection requests between any two nodes of the network. Each connection request has a unique identifier index number $R_i, i \in \mathbb{Z}_1^{\mathcal{N}}$ where $\mathbb{Z}_1^{\mathcal{N}} = \{1, \cdots, \mathcal{N}\}$ and $\mathcal{N}$ is the number of connection requests. A connection request is characterized by its bandwidth profile, which enforces limits on bandwidth utilization according to

the service level specification that has been agreed upon by the subscriber and the service provider as part of the SLA. The bandwidth profile is a 3-tuple $R_i = (\check{R}_i, \widetilde{R}_i, \widehat{R}_i)$ whose elements denote minimum, average, and maximum required transmission rate, respectively. The connection request R_i has a buffer queue where $q_i[n]$ denotes its backlog length in time slot n. The queue content of the connection request R_i is serviced by a connecting light-path which provides a number of $s_i[n]$ contiguous frequency slots to transmit backlogged packets. The queue $q_i[n]$ is filled by a constant arrival rate $a_i[n]$ during each time slot n. In fact, we assume that there is a traffic shaper that collects the input packets of a queue during time slot $n-1$ and delivers them to the queue at constant arrival rate $a_i[n]$ within time slot n [13]. Note that all the queueing processes occur at the edge nodes, thereby obviating the need for buffering in the intermediate optical cross-connects.

The light-path of connection request R_i can be routed over one of its available $\mathcal{K}$-shortest paths $P_i = (P_{i,1}, \cdots, P_{i,\mathcal{K}})$. The selected path is determined by a binary variable $x_{i,j}[n]$ that is 1 if connection request R_i uses path $P_{i,j}$ in time slot n and otherwise 0. Each path is characterized by its constituting links. Paths $P_{i,j}$ and $P_{i',j'}$ with at least one common link are named intersected paths and denoted by $P_{i,j} \cap P_{i',j'} \neq \varnothing$. There is a pair of transmit and receive transponders at the source and destination nodes of the light-path devoted to connection request R_i, which operates on contiguous frequency slots $f_i[n]$ to $f_i[n] + s_i[n] - 1$, where $f_i[n]$ is called the start frequency slot of time slot n. The short transmission distances of MEONs let transponders to use the modulation format with the highest bit per symbol value $\mathcal{M}$. Therefore, the contiguous frequency slots of $f_i[n]$ to $f_i[n]+s_i[n]-1$ provide a transmission rate of $\mathcal{MW}s_i[n]$ b/s in time slot n. For each connection request R_i, the transmission rate of the servicing light-path $\mathcal{MW}s_i[n]$ can fluctuate between the minimum and maximum values of $\check{R}_i$ and $\widehat{R}_i$, but its time-averaged rate should equal $\widetilde{R}_i$, as shown in Fig. 2. There should be at least $\mathcal{G}$ guard frequency slots between the assigned frequency slots of two transponders with intersected light-paths. The relative location of the start frequency slots is given by the boolean variable $t_{i,j}[n]$ that equals 1 if $f_i[n] \leqslant f_j[n]$, and 0 otherwise. $u[n]$ is an upper bound on the maximum index of the used frequency slots in time slot n. We minimize this upper bound during the resource allocation optimization process to tighten the bound and squeeze the assigned frequency slots. Therefore, the tight upper bound value of $u[n]$ accurately estimates the maximum index of the used frequency slots in time slot n and can be used to quantize the amount of spectrum usage in each time slot.

There is a centralized SDN controller that runs the pipeline process of Fig. 3. The pipeline includes the three stages of check, run, and config, where each stage should complete its process within the duration of a time slot $\mathcal{T}$. In the check stage, the controller queries optical nodes to check and update queue backlog and arrival state information. During the run stage, the controller runs a resource allocation algorithm in which network status information is used to allocate network resources, route light-paths and calculate the new configuration

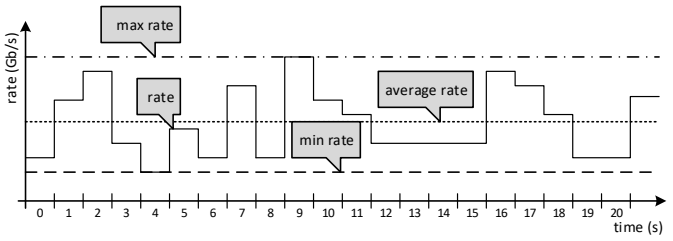

Fig. 2: A sample bandwidth profile with its characterizing parameters.

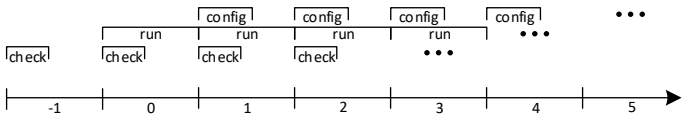

Fig. 3: Controller pipeline process with three stages of check, run, and config.

of the transponders. Finally in the config stage, the controller sends command messages to reconfigure transponders. The check time mainly depends on the signal propagation delay in the control plane while the duration of the config stage relates to the transponder reconfiguration and switching time. The run time, which has the dominant duration, is equal to the convergence time of the resource allocation algorithm. Noting the dynamic behavior of the traffic in metro networks, we need a fast and online resource allocation algorithm to periodically adapt the available resources to the traffic demands with the least possible reallocation time interval. This is a new requirement which has not been addressed in previous resource allocation methods for conventional EONs.

The considered service model is sufficiently general to support various scenarios and transmission requirements. Although transmission delay is not included among the SLA describing parameters, the considered traffic profile is flexible enough to support different requirements on transmission delay. For instance, to carry a fixed-rate traffic stream with a forced delay constraint, we can sign an SLA on a bandwidth profile (r, r, r). Such a bandwidth profile provides a fixed transmission rate of r over time and guarantees instantaneous transmission of the data packets for arrival rates below r. As a more general case, consider a mixed traffic flow for which we need to send some certain packets instantaneously while the remaining packets can be buffered and transmitted in a proper time. Such a traffic flow can be modeled as a mixture of a fixed traffic stream with a fixed rate of r and a variable traffic stream with an average rate $\bar{r}$. Clearly, a bandwidth profile with specification parameters $(r, r + \bar{r}, \infty)$ can simply serve this mixed traffic pattern. Using this bandwidth profile, the fixed-rate part of the traffic is served without delay and the variable-rate part is queued and delayed such that the required average rate of $\bar{r}$ is obtained.

In the following, we define the parameters being used in the optical networking framework:

- Input parameters:
  1) $\mathbb{Z}_a^b = \{n \in \mathbb{Z} | a \leqslant n \leqslant b\}$: Set of integer numbers

between a and b, inclusively.
2) $\mathcal{T}$: Time slot width.
3) $\mathcal{B}$: Optical fiber bandwidth.
4) $\mathcal{W}$: Frequency slot bandwidth.
5) $\mathcal{F}$: Number of frequency slots.
6) $\mathcal{G}$: Minimum required guard frequency slots.
7) $\mathcal{M}$: Modulation bit per symbol.
8) $\mathcal{N}$: Number of connection requests.
9) $\mathcal{K}$: Number of candidate shortest paths.
10) $\mathcal{L}$: Lyapunov penalty coefficient.
11) $\mathbf{R} = \{R_i = (\check{R}_i, \widetilde{R}_i, \widehat{R}_i) | \check{R}_i \leqslant \widetilde{R}_i \leqslant \widehat{R}_i, i \in \mathbb{Z}_1^{\mathcal{N}}\}$: Set of connection requests. Connection request R_i is specified by its bandwidth profile $(\check{R}_i, \widetilde{R}_i, \widehat{R}_i)$ where $\check{R}_i$, $\widetilde{R}_i$, and $\widehat{R}_i$ are minimum, average, and maximum transmission rate, respectively.
12) $\mathbf{P} = \{P_i = (P_{i,1}, \cdots, P_{i,\mathcal{K}}) | i \in \mathbb{Z}_1^{\mathcal{N}}\}$: Set of $\mathcal{K}$ shortest available paths for connection request i. Each path is characterized by its constituting links.
13) $\mathbf{a}[n] = \{a_i[n] | i \in \mathbb{Z}_1^{\mathcal{N}}\}$: Arrival rate of connection request R_i in time slot n.

- Output parameters:
1) $\mathbf{q}[n] = \{q_i[n] | i \in \mathbb{Z}_1^{\mathcal{N}}\}$: Queue backlog of connection request R_i in time slot n.
2) $\mathbf{h}[n] = \{h_i[n] | i \in \mathbb{Z}_1^{\mathcal{N}}\}$: Virtual queue backlog of connection request R_i in time slot n.
3) $\mathbf{s}[n] = \{s_i[n] | i \in \mathbb{Z}_1^{\mathcal{N}}\}$: Number of servicing frequency slots of connection request R_i in time slot n.
4) $\mathbf{f}[n] = \{f_i[n] | i \in \mathbb{Z}_1^{\mathcal{N}}\}$: Positive integer variable which denotes the start frequency slot of connection request R_i in time slot n.
5) $\mathbf{x}[n] = \{x_{i,j}[n] | i \in \mathbb{Z}_1^{\mathcal{N}}, j \in \mathbb{Z}_1^{\mathcal{K}}\}$: Boolean variable that equals 1 if connection request R_i uses path $P_{i,j}$ in time slot n and otherwise 0.
6) $\mathbf{t}[n] = \{t_{i,j}[n] | i, j \in \mathbb{Z}_1^{\mathcal{N}}, i \neq j\}$: Auxiliary boolean variable that equals 1 if $f_i[n] \leqslant f_j[n]$, and 0 otherwise.
7) $u[n]$: An upper bound on the index of the occupied frequency slots in time slot n.

III. Proposed Solution

Fixed network planning does not consider the dynamic state of the traffic demands and allocates available resources for worst-case conditions [14]. Worst-case fixed resource allocation is the solution of the following ILP:

$$\min_{\mathbf{x},\mathbf{f},\mathbf{t},u} \; u \tag{1a}$$

$$f_i + \lceil \frac{\widehat{R}_i}{\mathcal{MW}} \rceil \leqslant u \leqslant \mathcal{F}, \quad \forall i \in \mathbb{Z}_1^{\mathcal{N}} \tag{1b}$$

$$\sum_{j=1}^{\mathcal{K}} x_{i,j} = 1, \quad \forall i \in \mathbb{Z}_1^{\mathcal{N}} \tag{1c}$$

$$t_{i,j} + t_{j,i} = 1, \quad \forall i, j \in \mathbb{Z}_1^{\mathcal{N}} : i \neq j \tag{1d}$$

$$f_i + \lceil \frac{\widehat{R}_i}{\mathcal{MW}} \rceil + \mathcal{G} \leqslant f_j + \mathcal{F}(3 - t_{i,j} - x_{i,k} - x_{j,l}), \quad \forall i, j \in \mathbb{Z}_1^{\mathcal{N}}, \forall k, l \in \mathbb{Z}_1^{\mathcal{K}} : i \neq j, P_{i,k} \cap P_{j,l} \neq \varnothing \tag{1e}$$

where the optimization is over the time-independent discrete variable sets $\mathbf{x}$, $\mathbf{f}$, and $\mathbf{t}$ and the scalar variable u. We minimize the upper bound u in the objective function (1a) to squeeze the assigned frequency slots to the left side of the fiber spectrum band and free up its right side for the incoming connection requests. Constraint (1b) limits the index of the end frequency slots to its upper bound u such that the assigned contiguous bandwidth includes $\lceil \frac{\widehat{R}_i}{\mathcal{MW}} \rceil$ frequency slots to support the maximum transmission rate $\widehat{R}_i$. In (1b), $\lceil . \rceil$ is the ceiling function, which returns the least integer greater than or equal to its argument. Constraint (1c) specifies that only one path should be assigned to each request. Constraint (1d) determines the relative location of the assigned spectrum bandwidths of any two connection requests. Finally, constraint (1e) specifies that the adjacent spectrum bandwidths of a link should be separated by more than $\mathcal{G}$ guard frequency slots. Note that formulation (1) assigns the spectrum bandwidths for the maximum required transmission rates, and hence its solution provides an over-provisioned network configuration.

Data streams in metro networks appear as bursts of traffic with high peak to average values and diverse durations. To meet the worst-case traffic condition in formulation (1), it is necessary to allocate spectrum bandwidths for the peaks of traffic bursts. This leads to an inefficient resource utilization, since in many time intervals, there is not sufficient traffic volume to completely fill the fixed allocated spectrum bandwidths. The solution is to provide an adaptation between the allocated resources and temporal behavior of traffic flows, which is addressed in formulation (2):

$$\min_{\mathbf{x}[n],\mathbf{f}[n],\mathbf{t}[n],\mathbf{s}[n],u[n]} \bar{u} = \lim_{n\to\infty} \frac{1}{n} \sum_{m=0}^{n-1} \mathbb{E}\{u[m]\} \tag{2a}$$

$$\lim_{n\to\infty} \frac{\mathbb{E}\{q_i[n]\}}{n} = 0, \quad \forall i \in \mathbb{Z}_1^{\mathcal{N}} \tag{2b}$$

$$\mathcal{MW}\bar{s_i} = \lim_{n\to\infty} \frac{\mathcal{MW}}{n} \sum_{m=0}^{n-1} \mathbb{E}\{s_i[m]\} = \widetilde{R}_i, \quad \forall i \in \mathbb{Z}_1^{\mathcal{N}} \tag{2c}$$

$$\lfloor \frac{\check{R}_i}{\mathcal{MW}} \rfloor \leqslant s_i[n] \leqslant \lceil \frac{\widehat{R}_i}{\mathcal{MW}} \rceil, \quad \forall i \in \mathbb{Z}_1^{\mathcal{N}}, \forall n \in \mathbb{Z}_0^{\infty} \tag{2d}$$

$$f_i[n] + s_i[n] \leqslant u[n] \leqslant \mathcal{F}, \quad \forall i \in \mathbb{Z}_1^{\mathcal{N}}, \forall n \in \mathbb{Z}_0^{\infty} \tag{2e}$$

$$\sum_{j=1}^{\mathcal{K}} x_{i,j}[n] = 1, \quad \forall i \in \mathbb{Z}_1^{\mathcal{N}}, \forall n \in \mathbb{Z}_0^{\infty} \tag{2f}$$

$$t_{i,j}[n] + t_{j,i}[n] = 1, \quad \forall i, j \in \mathbb{Z}_1^{\mathcal{N}}, \forall n \in \mathbb{Z}_0^{\infty} : i \neq j \tag{2g}$$

$$f_i[n] + s_i[n] + \mathcal{G} \leqslant f_j[n] + \mathcal{F}(3 - t_{i,j}[n] - x_{i,k}[n] - x_{j,l}[n]), \quad \forall i, j \in \mathbb{Z}_1^{\mathcal{N}}, \forall k, l \in \mathbb{Z}_1^{\mathcal{K}}, \forall n \in \mathbb{Z}_0^{\infty} : i \neq j, P_{i,k} \cap P_{j,l} \neq \varnothing \tag{2h}$$

where $\mathbf{x}[n]$, $\mathbf{f}[n]$, $\mathbf{t}[n]$, and $\mathbf{s}[n]$ are variable sets of path identifier, start frequency slot, spectrum relative location, and number of servicing frequency slots in time slot n, while $u[n]$ denotes the upper bound on the index of the occupied

frequency slots within time slot n. The goal function (2a) aims at the minimization of the time-averaged spectrum usage, where the expectation is over the randomness of the network variables. The stability constraint (2b) states that queues should have finite length in the sense of mean-rate stability [13]. Constraint (2c) is added to guarantee the specified average transmission rate of each connection request, while constraint (2d) holds the number of servicing frequency slots between its allowed minimum and maximum values. In (2d), $\lfloor . \rfloor$ is the floor function, which returns the greatest integer less than or equal to its argument. The other constraints are similar to their corresponding counterparts in formulation (1), except that they should be satisfied in each time slot for adaptive values of the number of servicing frequency slots $s_i[n]$, not for the worst-case maximum transmission rates. The optimization problem (2) can be viewed as a stochastic integer program, where queue arrivals are its main random events. Note that the problem may include more constraints to describe other system limitations and/or operator requirements. For example, if an operator needs to keep a continuity property for the routing, we can simply add a constraint such as $x_{i,j}[n] = x_{i,j}[0], \quad \forall i \in \mathbb{Z}_1^{\mathcal{N}}, \forall j \in \mathbb{Z}_1^{\mathcal{K}}, \forall n \in \mathbb{Z}_1^{\infty}$ to keep routes unchanged during time. Moreover, such continuity constraints fix part of the optimization variables and consequently, reduce the computational complexity and convergence time. The optimization problem (2) is a purely theoretical construction, which jointly optimizes the variables for all $n \in \mathbb{Z}_0^{\infty}$. We need the future state of the network to solve (2) and this is not possible for a practical and causal implementation. Even if we truncate (2) to a finite number of time slots with known state information, the resulting complexity and delay will be too large for deployment in practice. We therefore approximate the solution of (2) using a causal and sequential algorithm, which optimizes the variables in each time slot and follows a dynamic state line to achieve the optimum value of the time-averaged objective function.

The elegant theory of Lyapunov drift optimization can be used to handle time-averaged objective function and constraints of the stochastic optimization problem (2). In Lyapunov optimization, a penalty term, which is called Lyapunov function and is a scalar measure of the network congestion state, is added to the goal function and the solution of the problem is derived using Min-Drift-Plus-Penalty algorithm [13]. According to this algorithm, we observe the current queue states $q_i[n]$ and the random arrivals $a_i[n]$ and solve the following ILP in each time slot n sequentially:

$$\min_{\mathbf{x}[n],\mathbf{f}[n],\mathbf{t}[n],\mathbf{s}[n],u[n]} \mathcal{L}u[n] + \mathcal{T}\sum_{i=1}^{\mathcal{K}} q_i[n](a_i[n] - \mathcal{M}\mathcal{W}s_i[n])$$

$$+ \mathcal{T}\sum_{i=1}^{\mathcal{K}} h_i[n](\widetilde{R}_i[n] - \mathcal{M}\mathcal{W}s_i[n]) \tag{3a}$$

$$\lfloor \frac{\breve{R}_i}{\mathcal{M}\mathcal{W}} \rfloor \leqslant s_i[n] \leqslant \lceil \frac{\widehat{R}_i}{\mathcal{M}\mathcal{W}} \rceil, \quad \forall i \in \mathbb{Z}_1^{\mathcal{N}} \tag{3b}$$

$$f_i[n] + s_i[n] \leqslant u[n] \leqslant \mathcal{F}, \quad \forall i \in \mathbb{Z}_1^{\mathcal{N}} \tag{3c}$$

$$\sum_{j=1}^{\mathcal{K}} x_{i,j}[n] = 1, \quad \forall i \in \mathbb{Z}_1^{\mathcal{N}} \tag{3d}$$

$$t_{i,j}[n] + t_{j,i}[n] = 1, \quad \forall i,j \in \mathbb{Z}_1^{\mathcal{N}} : i \neq j \tag{3e}$$

$$f_i[n] + s_i[n] + \mathcal{G} \leqslant f_j[n] + \mathcal{F}(3 - t_{i,j}[n] - x_{i,k}[n] - x_{j,l}[n]), \quad \forall i,j \in \mathbb{Z}_1^{\mathcal{N}}, \forall k,l \in \mathbb{Z}_1^{\mathcal{K}} : i \neq j, P_{i,k} \cap P_{j,l} \neq \varnothing \tag{3f}$$

where $\mathcal{L}$ is named Lyapunov penalty coefficient and $h_i[n], i \in \mathbb{Z}_1^{\mathcal{N}}$ is called virtual queue length. After (3) is solved for a given value of n, we update real and virtual queue backlogs according to:

$$h_i[n+1] = h_i[n] + \mathcal{T}(\widetilde{R}_i[n] - \mathcal{M}\mathcal{W}s_i[n]), \quad \forall i \in \mathbb{Z}_1^{\mathcal{N}} \tag{4}$$

$$q_i[n+1] = \max\{q_i[n] - \mathcal{T}\mathcal{M}\mathcal{W}s_i[n], 0\} + \mathcal{T}a_i[n], \quad \forall i \in \mathbb{Z}_1^{\mathcal{N}} \tag{5}$$

Thereafter, n is incremented and (3) is solved again. $h_i[0]$ can be initialized by a value of 0 while $q_i[0]$ denotes the backlog length of queue i in reference time slot 0. According to the Lyapunov drift optimization theory, time-averaged constraints can be handled using the same way as the queue stability constraints. As a result, a virtual queue is assigned to each time-averaged constraint and is updated using a similar recursive update equation. As proven in [13], there is a trade-off between solution optimality and queue backlogs in the Lyapunov optimization technique, which can be adjusted by the coefficient $\mathcal{L}$. Clearly, this translates to an equivalent trade-off between spectrum usage and transmission delay for the formulated optimization problem. Higher values of $\mathcal{L}$ give more weight to the spectrum usage in the optimization problem (3) while its lower values increase the priority of the queue servicing and hence, reduce the transmission delay. For a detailed discussion about the Lyapunov optimization theory, the interested reader can refer to [13]. Formulation (3) is an ILP and its solution can be easily derived using well-known algorithms such as the simplex method, branch and bound algorithm, or cutting plane technique. Such algorithms have been implemented in reputable software packages such as CPLEX and Gurobi.

IV. Numerical Results

In this section, we use simulation results to demonstrate the performance of the proposed dynamic resource allocation procedure. We use the metro network topology of Fig. 4 as our test network. This network topology, which is an adapted version from a real industrial network, has been also used in [2] as a good sample for metro network simulation. The network operates over the C band whose bandwidth $\mathcal{B} = 4$ is divided into $\mathcal{F} = 640$ frequency slots with a fixed bandwidth of $\mathcal{W} = 6.25$ GHz. Transponders use polarization multiplexed quadrature phase shift keying (PM-QPSK) with $\mathcal{M} = 4$ bits per symbol. The number of guard frequency slots is $\mathcal{G} = 1$ [2], [14], [15]. The time slot width is set to $\mathcal{T} = 5$ s which is an acceptable value for fast dynamic resource allocation [12]. The ring- and chain-shaped parts of the network topology show core and aggregation segments, respectively.

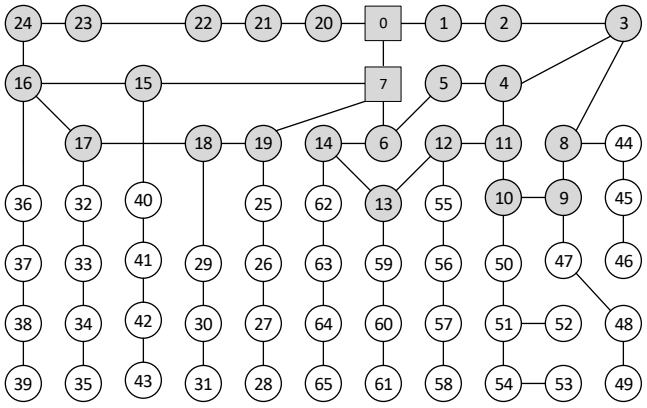

Fig. 4: A sample metro elastic optical network with 66 optical nodes and 70 fiber links. Core rings and aggregation chains are shown by dark and bright nodes, respectively. Nodes 0 and 7 are backbone core nodes.

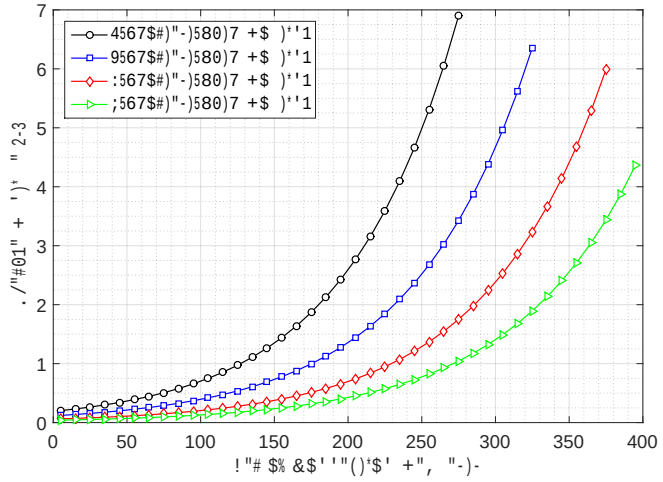

Fig. 5: Runtime versus number of connection requests for various numbers of candidate shortest paths in the $\mathcal{K}$-shortest path algorithm.

In the aggregation segment, traffic flows are aggregated from dispersed metro access nodes to their associated metro core nodes and the latter further forward the aggregated traffic flows to the backbone metro core nodes. In our simulations, we use random values for bandwidth profile parameters of a typical connection request R_i. We first assign a random value from a uniform distribution over $[0, 40]$ Gb/s ($[0, 100]$ Gb/s in the core segment) to $\breve{R}_i$. Then, we set $\hat{R}_i$ to another uniformly-distributed random value from $[\breve{R}_i, 40]$ Gb/s ($[\breve{R}_i, 100]$ Gb/s in the core segment). Finally, we assign a random number to $\tilde{R}_i$, which is uniformly selected from $[\breve{R}_i, \hat{R}_i]$. We evaluate the performance of the technique under dynamic traffic load where the connection request generation rate between a node pair follows a Poisson process with mean $\mu_i, i \in \mathbb{Z}_1^{\mathcal{N}}$. The holding time of each established connection takes values from a negative exponential distribution with mean $\tau_i, i \in \mathbb{Z}_1^{\mathcal{N}}$ and the transmission rate of each connection demand is uniformly

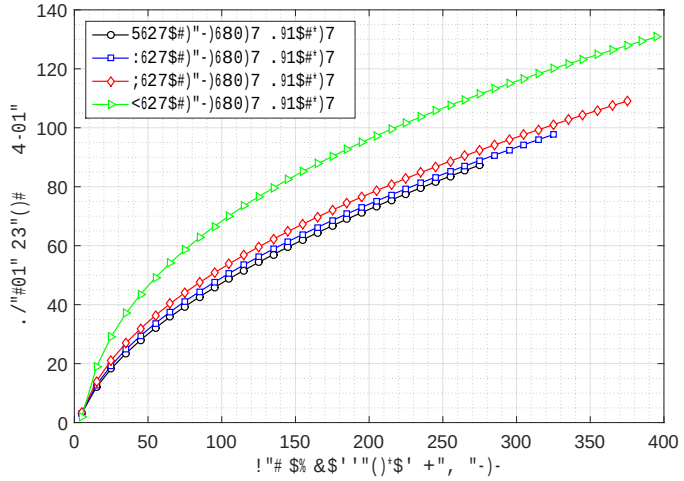

Fig. 6: Spectrum usage versus number of connection requests for various numbers of candidate shortest paths in the $\mathcal{K}$-shortest path algorithm.

distributed over $[\breve{\nu}_i, \hat{\nu}_i]$ Gb/s with the mean value of $\nu_i, i \in \mathbb{Z}_1^{\mathcal{N}}$ [2]. We set $\breve{\nu}_i$, $\hat{\nu}_i$, and $\mu_i \tau_i \nu_i$ to the randomly selected values of $\breve{R}_i$, $\hat{R}_i$, and $\tilde{R}_i$, respectively. The values of μ_i are taken from a uniform distribution over $[0, 1]$. We use the MATLAB software for programming and simulation. The YALMIP and Gurobi optimization applications are also used for modeling and solving the proposed optimization problems. The simulations run on a computer equipped with a Intel Core i7-472HQ CPU and 8 GB of RAM.

To investigate the computational complexity of formulation (3), we report its average runtime versus the number of connection requests for various number of candidate shortest paths in the $\mathcal{K}$-shortest path algorithm. Fig. 5 shows that the runtime of the ILP is approximately an exponential function of the number of connection requests, where the exponent coefficient reduces for lower values of $\mathcal{K}$. Furthermore, the runtime is approximately doubled by adding one more path to the set of candidate shortest paths. Therefore, $\mathcal{K} = 1$ is a suitable choice, which can provide an acceptable level of practical scalability. For a larger network topology, we can use a more powerful computational platform to further reduce the runtime. The results show that the proposed algorithm can satisfy timing constraints in online resource allocation with a resource reallocation period of less than a few seconds and therefore, it offers a good potential for fast dynamic resource allocation in MEONs. The proposed formulation can be solved more than two orders of magnitude faster than its counterparts in backbone networks, where signal quality constraints of the long transmission fibers are the main source of the computational complexity [21], [22]. The proposed formulation is devoted to the metro networks with shorter transmission fibers and easier signal quality constraints and therefore, it has lower computational complexity and runtime.

Considering the tight upper bound value of $u[n]$ as an indicator of spectrum usage in time slot n, Fig. 6 reports the average spectrum usage versus number of connection requests for

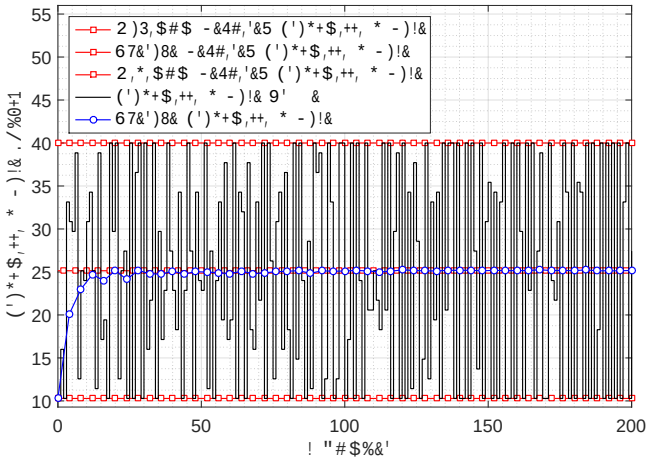

(a) A sample connection request with bandwidth profile $(10, 25, 40)$ Gb/s.

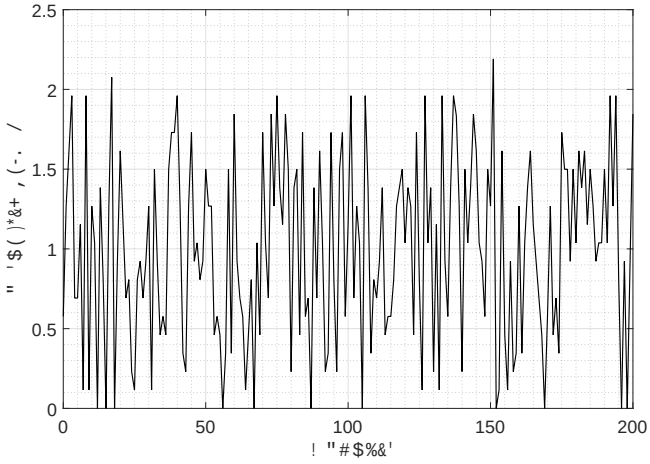

(b) A sample connection request with bandwidth profile $(10, 25, 40)$ Gb/s.

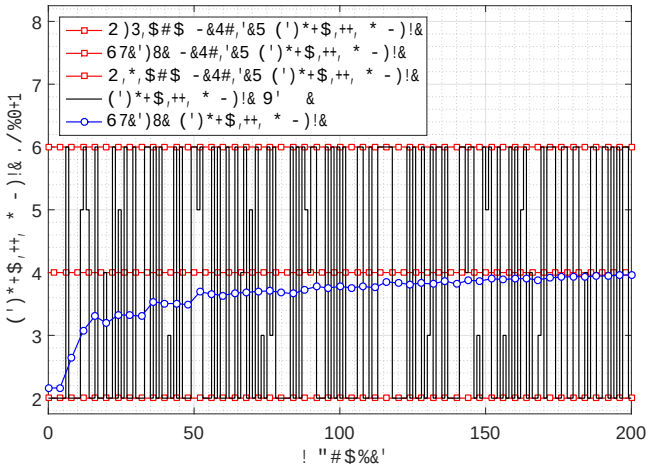

(c) A sample connection request with bandwidth profile $(2, 4, 6)$ Gb/s.

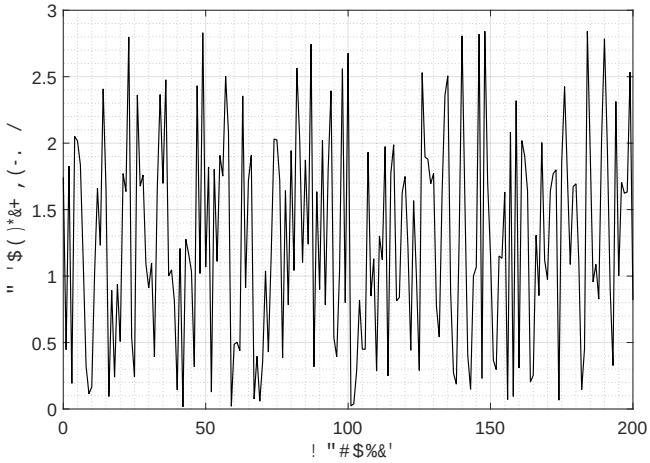

(d) A sample connection request with bandwidth profile $(2, 4, 6)$ Gb/s.

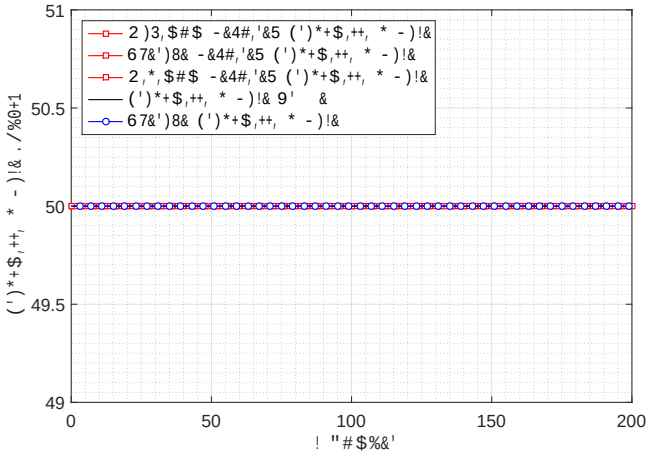

(e) A sample connection request with bandwidth profile $(50, 50, 50)$ Gb/s.

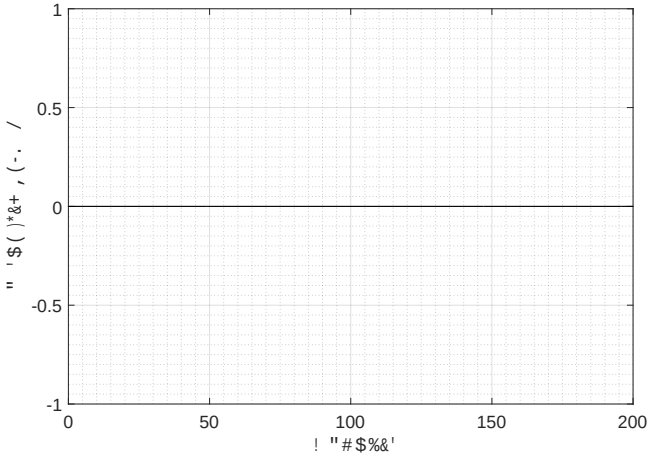

(f) A sample connection request with bandwidth profile $(50, 50, 50)$ Gb/s.

Fig. 7: Bandwidth profile and normalized backlog versus time slot for three sample connection requests.

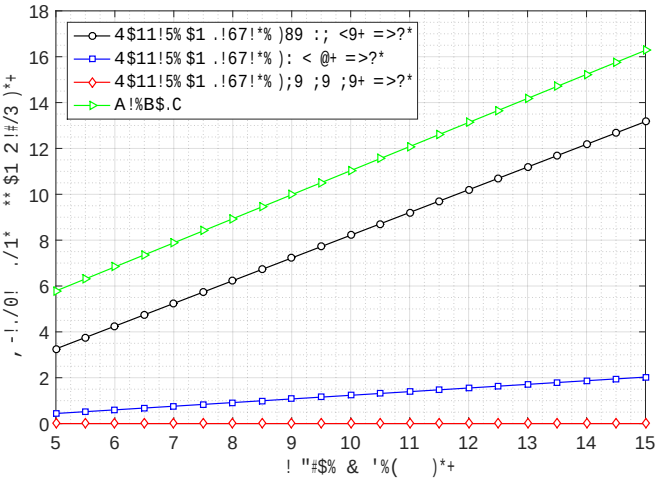

Fig. 8: Average transmission delay versus time slot width for the network and three sample connection requests.

various numbers of candidate shortest paths in the $\mathcal{K}$-shortest path algorithm. Spectrum usage is an ascending function of the number of connection requests. Dynamic behavior of the traffic flows may lead to spectrum fragmentation throughout the network. Our adaptive algorithm periodically reallocates the available resources according to the current status of the network and traffic flows to defragment and squeeze the assigned spectrum widths. This defragmentation reduces the increasing slope of the spectrum usage curve for higher number of connection requests in Fig. 6. An important point is that spectrum usage decreases by increasing the number of candidate shortest paths $\mathcal{K}$, but there is no considerable gain for $\mathcal{K} > 2$. On the other hand, increasing $\mathcal{K}$ severely delays convergence of the optimization algorithm, as shown in Fig. 5. This implies that $\mathcal{K} = 2$ is a good choice, which provides an acceptable level of solution optimality in a short time.

A main contribution of the proposed resource allocation technique is its capability to support a wide range of service profiles. To demonstrate this feature, we select three sample connection requests among all the available connection requests and fix their bandwidth profiles to $(10, 25, 40)$, $(2, 4, 6)$, and $(50, 50, 50)$ Gb/s. We use simulation results to investigate transmission profiles, normalized backlogs and transmission delays of the three fixed bandwidth profiles in Figs. 7 and 8. To simultaneously capture the initial transient and steady state behaviors of the curves, we focus on time slots below 200. The normalized backlog is defined as the ratio of the queue backlog in time slot n to its time-averaged value and is an indicator of the network queue stability. As illustrated in Figs. 7a and 7b, the transmission rate of the first connection request fluctuates between its boundary limits such that its time average approaches the specified average transmission rate and its queue backlog remains finite. To satisfy stability constraint (2b), the optimization process maintains the maximum normalized queue backlog finite. The same statement holds for the second connection request with a narrower range of traffic fluctuation, as shown in Figs. 7c and 7d. A special case is the third connection request, in which all the bandwidth profile elements are equal. In Fig. 7e, the resource allocation algorithm provides a fixed transmission rate of 50 Gb/s for the third connection request. If the input packets of the third connection request arrive by a fixed arrival rate less than 50 Gb/s, there is no backlogged packet and buffering delay in the queue, as shown in Fig. 7f. We report the absolute values of the average transmission delay versus time slot width for the three considered sample requests in Fig. 8. The transmission delay is approximately a linear function of the time slot width with a slope value that depends on the bandwidth profile parameters. Clearly, there is no transmission delay for the fixed-rate connection request while the two other traffic requests, which have wider ranges of traffic fluctuation, experience more transmission delay. This implies that we should sign an SLA for a bandwidth profile with a narrower range of traffic fluctuation to support a traffic flow with strict transmission delay requirements. For the considered network topology and random values of the traffic bandwidth parameters, the average network transmission delay can be less than 6 s. Undoubtedly, one can reduce the average network transmission delay by reducing the fluctuation range of the bandwidth profile parameters and/or time slot width $\mathcal{T}$. As shown in Fig. 8, a high value of $\mathcal{T}$ can unacceptably increase the average network transmission delay and make the network control process unstable.

To demonstrate the performance of the proposed resource allocation technique, we compare its results with the fixed resource allocation formulation (1), in which the resources are assigned for the maximum transmission rates of the connection requests. The spectrum usage ratio is defined as the ratio of the spectrum usage for the proposed resource allocation technique to its corresponding value for the fixed resource allocation scheme. Clearly, lower values of the spectrum usage ratio is desired. Fig. 9a shows a sample curve of the spectrum usage ratio versus time slot in which the values are less than 0.75 for all time slots. This implies that the spectrum usage of the proposed technique is less than 75% of the fixed resource allocation scheme over all time slots. The time-average of the spectrum usage ratio is approximately 0.62 for this sample curve, which shows that on average, the proposed technique reduces spectrum usage by a factor of 38%. Unlike the traditional fixed resource allocation, the proposed technique considers the instantaneous behavior of the network for spectrum assignment and therefore, it reduces the assigned spectrum widths in low traffic time slots. We also report the corresponding value of the normalized total backlog for this sample scenario. Clearly, normalized total backlog values are upper-limited by 1.25, which means that the length of packet queues are finite in the entire network.

The improvement of the presented dynamic resource allocation algorithm is a function of the traffic fluctuation, which is determined by peak to average traffic ratio. The average spectral efficiency, which is defined as the time-averaged ratio of the total traffic demand transmission rate to the spectrum usage can be used as a performance metric to quantify the expected improvement of the resource allocation algorithm.

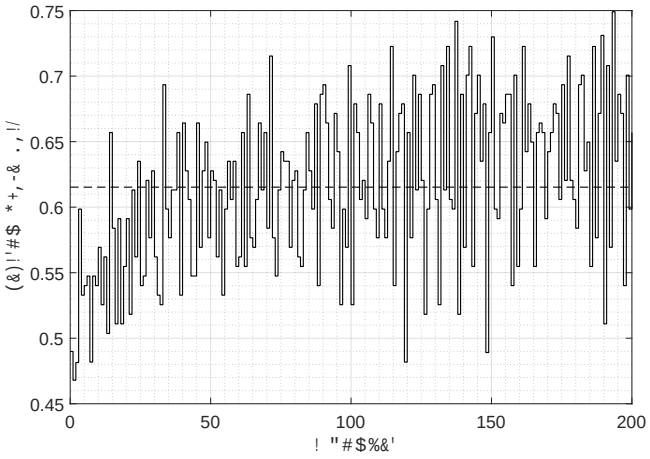

(a) The ratio between the spectrum usage of the proposed scheme and that of fixed allocation.

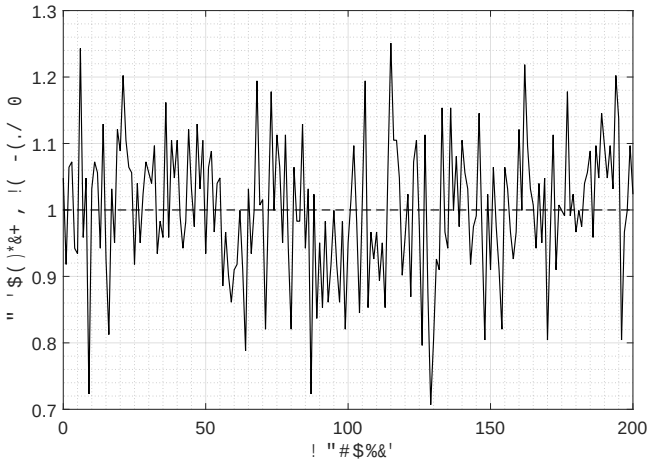

(b) Normalized total backlog versus time slot.

Fig. 9: Performance comparison of the proposed resource allocation technique with its fixed resource allocation counterpart.

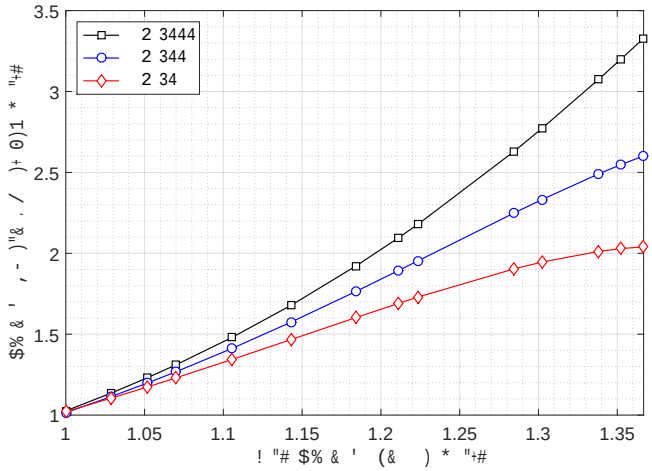

(a) The ratio between the spectral efficiency of the proposed scheme and that of fixed allocation.

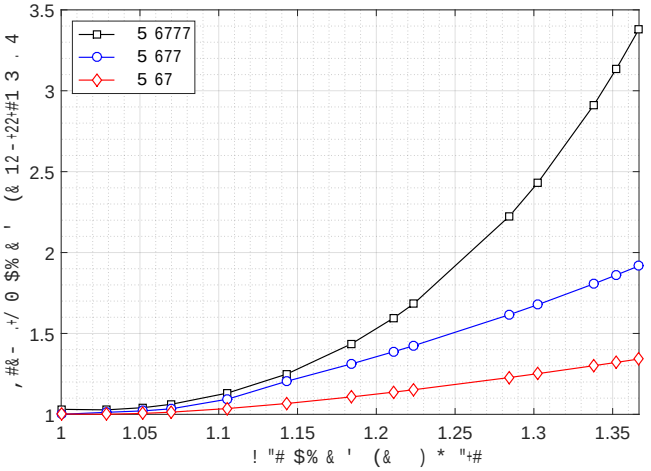

(b) Normalized transmission delay versus peak to average traffic ratio.

Fig. 10: Trade-off between transmission delay and spectrum utilization in the proposed resource allocation technique.

To provide a comparison, we report the ratio of the average spectral efficiency of our algorithm to its corresponding value for fixed resource allocation scheme in Fig. 10a. Clearly, our algorithm is more capable to utilize spectrum and it can improve spectral efficiency by a factor of 3.3 for a peak to average traffic ratio of 1.37 and a Lyapunov penalty coefficient $\mathcal{L} = 10^3$. There is a trade-off between solution optimality and queue backlog in the Lyapunov optimization technique which is a function of the Lyapunov penalty coefficient $\mathcal{L}$ [13]. This trade-off translates to an equivalent compromise between spectral efficiency and transmission delay in formulation (3). Figs. 10a and 10b show average spectral efficiency ratio and normalized average transmission delay versus peak to average traffic ratio for the Lyapunov penalty coefficients $\mathcal{L} = 10$, 10^2, and 10^3. The normalized average transmission delay equals the ratio of the average transmission delay to its corresponding value for a peak to average traffic ratio of 1 and a Lyapunov penalty coefficient of $\mathcal{L} = 10$. As shown in the figures, increasing $\mathcal{L}$ increases the transmission delay while the spectral efficiency also increases, which means that one can reduce spectrum usage at the cost of adding more transmission delay to the queued packets.

V. Conclusion

We use Lyapunov optimization theory to propose an efficient resource allocation algorithm for the dynamic resource management in metro elastic optical networks. The proposed algorithm provides an adaptation between network resources

and dynamic behavior of traffic demands to meet the requested service level agreement of each traffic source. The heart of the algorithm is a stochastic optimization problem that aims at minimizing the time-averaged spectrum usage constrained to specified service level requirements and physical restrictions. Lyapunov drift optimization theory can be used to derive the solution of the proposed stochastic optimization formulation, which is an integer linear program that is periodically solved to create an adaptation between allocated resources and traffic demand state information. Simulation results show that the proposed resource allocation technique can be used in online resource allocation with a reallocation period of less than a few seconds. Furthermore, it drastically improves spectral efficiency compared to a fixed network planning scheme (more than 230% improvement in a typical scenario). The amount of improvement is more if the service level agreements can tolerate more transmission delay.

REFERENCES

[1] P. Layec *et al.*, "Will metro networks be the playground for (true) elastic optical networks?" *Journal of Lightwave Technology*, vol. 35, no. 6, pp. 1260–1266, 2017.

[2] G. Shen *et al.*, "Ultra-dense wavelength switched network: A special EON paradigm for metro optical networks," *IEEE Communications Magazine*, vol. 56, no. 2, pp. 189–195, 2018.

[3] Bell Labs Consulting, "Metro network traffic growth: an architecture impact study," *https://www.tmcnet.com/tmc/whitepapers/documents/whitepapers/2013/9378-bell-labs-metro-network-traffic-growth-an-architecture.pdf*, Online; accessed 3 March 2019.

[4] W. Lautenschlaeger *et al.*, "Optical ethernet—flexible optical metro networks," *Journal of Lightwave Technology*, vol. 35, no. 12, pp. 2346–2357, 2017.

[5] Cisco, "Cisco global cloud index: Forecast and methodology, 2016–2021," *https://www.cisco.com/c/en/us/solutions/collateral/service-provider/global-cloud-index-gci/white-paper-c11-738085.html*, Online; accessed 3 March 2019.

[6] V. López and L. Velasco, *Elastic Optical Networks*. Springer, 2016.

[7] A. S. Thyagaturu *et al.*, "Software defined optical networks (SDONs): A comprehensive survey," *IEEE Communications Surveys & Tutorials*, vol. 18, no. 4, pp. 2738–2786, 2016.

[8] A. Dupas *et al.*, "Ultra-fast hitless 100Gbit/s real-time bandwidth variable transmitter with SDN optical control," in *Optical Fiber Communication Conference (OFC)*, 2018, pp. Th2A–46.

[9] C. Rottondi *et al.*, "On the benefits of elastic transponders in optical metro networks," in *Optical Fiber Communication Conference and National Fiber Optic Engineers Conference (OFC/NFOEC)*, 2012.

[10] A. Dupas *et al.*, "Elastic optical interface with variable baudrate: Architecture and proof-of-concept," *IEEE/OSA Journal of Optical Communications and Networking*, vol. 9, no. 2, pp. A170–A175, 2017.

[11] ——, "Hitless 100 Gbit/s OTN bandwidth variable transceiver for software-defined networks," in *Optical Fiber Communication Conference (OFC)*, 2016.

[12] L. Zhang and V. Chan, "Scalable fast scheduling for optical flow switching using sampled entropy and mutual information broadcast," *IEEE/OSA Journal of Optical Communications and Networking*, vol. 6, no. 5, pp. 459–475, 2014.

[13] M. J. Neely, "Stochastic network optimization with application to communication and queueing systems," *Synthesis Lectures on Communication Networks*, vol. 3, no. 1, pp. 1–211, 2010.

[14] B. C. Chatterjee *et al.*, "Routing and spectrum allocation in elastic optical networks: A tutorial," *IEEE Communications Surveys & Tutorials*, vol. 17, no. 3, pp. 1776–1800, 2015.

[15] M. Hadi and M. R. Pakravan, "Resource allocation for elastic optical networks using geometric optimization," *IEEE/OSA Journal of Optical Communications and Networking*, vol. 9, no. 10, pp. 889–899, 2017.

[16] ——, "Energy-efficient fast configuration of flexible transponders and grooming switches in OFDM-based elastic optical networks," *IEEE/OSA Journal of Optical Communications and Networking*, vol. 10, no. 2, pp. 90–103, 2018.

[17] W. Gao and M. Cvijetic, "Allocation of spectral and spatial modes in multidimensional metro-access optical networks," *Optics Communications*, vol. 413, pp. 80–86, 2018.

[18] A. X. Zheng *et al.*, "Metropolitan area network architecture for optical flow switching," *IEEE/OSA Journal of Optical Communications and Networking*, vol. 9, no. 6, pp. 511–523, 2017.

[19] Q. She *et al.*, "Metro transport, from mesh to hub," in *Optical Fiber Communication Conference (OFC)*, 2017, pp. M2G–6.

[20] A. Triki *et al.*, "Carrier-grade performance evaluation in reliable metro networks based on optical packet switching," in *International Conference on Computing, Networking, and Communications (ICNC)*, 2017, pp. 70–75.

[21] L. Yan *et al.*, "Resource allocation for flexible-grid optical networks with nonlinear channel model [invited]," *Journal of Optical Communications and Networking*, vol. 7, no. 11, pp. B101–B108, 2015.

[22] M. Hadi and M. R. Pakravan, "Energy-efficient service provisioning in inter-data center elastic optical networks," *IEEE Transactions on Green Communications and Networking*, 2018.